ASM Sc. J., 20(2), 2025
https://doi.org/10.32802/asmscj.2025.1521

Study of Ti and Cr Co-doping for Improved Performance of Lithium Rich Li_2RuO_3 Cathode: A DFT+U Quantum Mechanical Study

C. Bapanayya[1,2*], G. Giribabu[3], G. Srinu[2] and R.P. Vijayalakshmi[1]

[1]*Department of Physics, S.V. University, Tirupati-517001, Andhra Pradesh, India*
[2]*Department of Physics, S.V.A. Govt. College, Srikalahasti-517644, Andhra Pradesh, India*
[3]*Government Degree College, Eluru – 534001, Andhra Pradesh, India*

Because of their high energy density and reversible capacity, lithium-rich layered oxides based on Ru, such as Li_2RuO_3 (LRO), are excellent candidates for use as cathodes in lithium-ion batteries. However, their commercial viability is limited due to poor structural stability, thermal instability, and voltage decay. Recent studied show that doping of Ti and Cr is a promising approach to resolve the structural stability and voltage losses associated with LRO cathodes. In this paper, we report DFT+U quantum mechanical studies on the Ti and Cr co-doping of LRO to achieve excellent and stable battery performance. We also investigated the impact of Ti to Cr doping ratio on the LRO battery cathode performance. Ti and Cr co-doped LRO cathodes exhibited superior performance over the pristine LRO in terms of structural, thermal and voltage stability. Over 1.7% increase in open circuit voltage, ≥ 9.8% increase in bandgap, and 35.9% reduction in voltage drop is observed for co-doped LRO cathodes compared to the pristine cathode. The results show that, among the various stoichiometric combinations of LRO cathodes, $Li_2Ru0.5Ti0.375Cr0.125O_3$ has the best performance with a formation energy of -15.10 eV, open circuit voltage of 4.35V and band gap of 0.33 eV.

Key words: Li_2RuO_3; Ti and Cr co-doping; DFT+U; Li-ion battery cathode

I. INTRODUCTION

Due to their portability as a convenient energy source, lithium-ion batteries (LIBs) are becoming increasingly common in electronic gadgets (Lu *et al.*, 2013). Because battery technology is becoming progressively important, there is an increasing demand for LIBs with higher electrochemical performance (Kalantarian *et al.*, 2013; Xu *et al.*, 2015; Ye *et al.*, 2014). For application in EVs and HEVs, more advanced LIBs (Li *et al.*, 2015; Song *et al.*, 2015) with enhanced electrochemical properties are required as opposed to commercially available cathode materials such as $LiNi_xMn_yCo_{1-x-y}O_2$, $LiFePO_4$, and $LiCoO_2$ (Liu *et al.*, 2017; Mizushima *et al.*, 1981; Padhi, 1997), which have drawbacks like capacity loss and low energy density. Therefore, much work has been done (Afyon *et al.*, 2013; Johnson *et al.*, 2010; Okumura *et al.*, 2014; J. Wang *et al.*, 2018) to identify the ideal cathode material. Due to their superior energy density and capacity retention, lithium-rich layered oxides, specifically Li_2MO_3 (M stands for transition metal), show enormous potential as cathode materials (Lanjan *et al.*, 2020a).

Li_2MO_3 consists of higher proportion of Li ions for intercalation/deintercalation increasing the capacity for reversible discharge (e.g., for Li_2MnO_3 discharge capacity is 460 $mAhg^{-1}$) (Lanjan *et al.*, 2020a). The cumulative anionic and cationic redox processes that lead to higher capacity are

*Corresponding author's e-mail: bapanayya@svagovtcm.ac.in

expected to be the cause of improved energy density of the Li_2MO_3 cathodes. Intercalation and deintercalation processes, however, stimulate the development of a spinel-like structure, which lowers intrinsic voltage and capacity (Su *et al.,* 2020*;* Wu *et al.*, 2020). Recent studies (Park *et al.*, 2013; S. Zheng *et al.*, 2019) have demonstrated that the monoclinic C2/c layered Li_2RuO_3 (LRO) cathode material outperforms other cathode materials in terms of reversibility of the oxygen extraction process during charge/discharge cycles. Additionally, modifications to the O-Li-O bond formation and Li-ion diffusion pathways could have an impact on the atomic configuration and cation ordering of this cathode material, which in turn could affect its electrochemical performance. Recent studies have shown that doping this cathode material significantly enhances its electrochemical characteristics. For instance, Arunkumar *et al.* (2016) found that the structural stability and reversibility of the cathode increased with increasing amounts of aliovalent Co^{3+} in lithium-rich LRO due to high cation ordering. Zheng *et al.* (2019) investigated the impact of Ni doping on the oxygen redox process in Li_2RuO_3 using first-principles calculations. Ni dopants were shown to significantly decrease the oxygen oxidation reaction, leading to an increase in capacity. Another group of researchers (Kalathil *et al.*, 2015) found that doping with Ti improves structural stability, Li-in diffusion, and electronic conductivity. Improved electrochemical performance has been observed in lithium-ion battery electrodes doped with Co (He *et al.*, 2019; Pang *et al.*, 2018; Yanxia *et al.*, 2020), Ni (Aasen *et al.*, 2020; Y. Zhang *et al.*, 2018), and Mg (Nkosi *et al.*, 2017; Torres-Castro *et al.*, 2017). In addition, Tian *et al.* (2019) investigated a co-doping method for LRO using Na and Cr elements. It has been observed that doping with Na increases voltage stability and that doping with Cr increases capacity. More recent studies by Moradi *et al.* (2021) show that co-doping of different transition metals (TMs) with Ti in undoped Li_2RuO_3 enhances maximum open circuit voltage, structural and thermodynamic stability, and decreases oxygen removal at the cathodes.

In this study, DFT+U quantum mechanical computations were used to examine the effects of co-doping Li_2RuO_3 (LRO) with Ti and Cr on its electrochemical properties. The elements Ti and Cr were chosen as co-dopants because of their ability to enhance the stability of crystal structure, reversibility, electrical conductivity, and theoretical capacity of un-doped LRO (Tian *et al.*, 2019; S. Zheng *et al.*, 2019). Important characteristics that affect the electrochemical performance of cathodes, such as formation energy, change in Gibb's free energy, open-circuit voltage, and bandgap, have been studied on co-doped cathodes using DFT+U quantum mechanics. The results of this study are anticipated to contribute to a deeper understanding of the effects of co-doping and development of multiple transition metal doped LRO cathode materials.

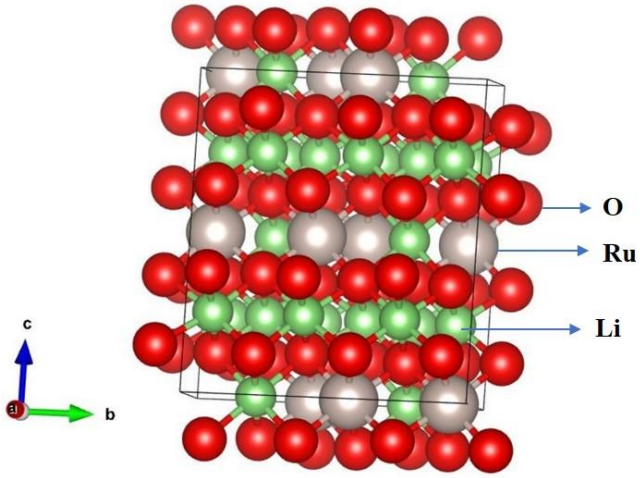

Figure 1. Unit cell of pristine Li_2RuO_3 containing layered structure of Li (green), Ru (grey) and O (red) atoms

II. COMPUTATIONAL METHODS

Li_2RuO_3 is a lithium-rich multi-layered oxide with a stable monoclinic structure (space group C2/c). Figure 1 displays a unit cell of pristine Li_2RuO_3 with 48 atoms of Ru, Li, and O atoms. Co-doped cathode materials were obtained by replacing half of the Ru atoms with the elements Ti and Cr. Using density functional theory, quantum mechanical computations were performed on pristine LRO and co-doped cathode materials (DFT). More reliable DFT+U (Lanjan *et al.*, 2020a; 2020b) technique, which uses the DFT theory to calculate energies while using Hubbard-U (Anisimov *et al.*, 1997) potentials for the transition metals (TMs) and PBE+U (Perdew *et al.*, 1996) as the exchange-correlation function was employed for all calculations in this study. Table 1 presents the Hubbard-U values used to correct the considerable correlation of d-orbitals in TM ions.

Table 1. Hubbard-U values of transition metals used in this study (Aryasetiawan *et al.*, 2006; Gao *et al.*, 2015; Wu *et al.*, 2020)

Transition Metal	Hubbard-U values (eV)
Ru	2.0
Ti	2.5
Cr	3.5

The experimental data of James *et al.* (1988) was used to find initial lattice parameters and atomic positions of un-doped LRO. The periodic crystal was represented by a $2 \times 2 \times 2$ supercell containing 48 atoms in each cell and all calculations were performed on this supercell. In all calculations, following convergence criteria were used: (i) the maximum energy for plane waves fixed at 500 eV and (ii) the energy convergence requirement of 10^{-4} eV/atom. In order to obtain the energetically favourable geometry, all atoms in the unit cell were completely relaxed. Subsequently, the co-doped cathodes were obtained by replacing one half of Ru atoms with Ti and Cr elements. The powder X-ray diffraction (XRD) was used to observe the structural alterations caused by doping. The powder XRD patterns of the cathodes were simulated using VESTA-3 visualisation tool (Momma & Izumi, 2011). The source of X-ray radiation was monochromatic Cu-K_α with a wavelength of 1.54059Å.

III. RESULTS AND DISCUSSION

A. Theoretical Capacity

The theoretical charge capacity of a cathode can be calculated using the following relationship (Zhi *et al.*, 2013):

$$Q_{theoretical} = \frac{nF}{3.6 \times MW} \quad (1)$$

where, n is the number of moles of Li in the cathode, F is the Faraday constant, and MW is the molecular weight of the cathode. For all the studied cathodes, the value of n is 2.

Table 2 displays the computed theoretical capacities of the cathodes. As shown in Table 2, co-doped cathodes have larger theoretical charge capacities than LRO cathodes. More precisely, $Li_2Ru_{0.5}Ti_{0.5}Cr_0O_3$, $Li_2Ru_{0.5}Ti_{0.375}Cr_{0.125}O_3$, $Li_2Ru_{0.5}Ti_{0.25}Cr_{0.25}O_3$, $Li_2Ru_{0.5}Ti_{0.125}Cr_{0.375}O_3$, and $Li_2Ru_{0.5}Ti_0Cr_{0.5}O_3$ have 19.5%, 19.1%, 18.6%, 18.2%, and 17.7% respectively, higher capacity than LRO (329.0 $mAhg^{-1}$). Among the studied cathodes, theoretical capacity is greatest for $Li_2Ru_{0.5}Ti_{0.5}Cr_0O_3$. The order of theoretical charge capacity ($Q_{theoretical}$) of the cathodes is:

$Li_2Ru_{0.5}Ti_{0.5}Cr_0O_3$ > $Li_2Ru_{0.5}Ti_{0.375}Cr_{0.125}O_3$ > $Li_2Ru_{0.5}Ti_{0.25}Cr_{0.25}O_3$ > $Li_2Ru_{0.5}Ti_{0.125}Cr_{0.375}O_3$ > $Li_2Ru_{0.5}Ti_0Cr_{0.5}O_3$ > Li_2RuO_3

Table 2. Theoretical charge capacities of co-doped cathodes and pristine Li_2RuO_3 and percentage change in the capacities

Cathode	$Q_{theoretical}$ ($mAhg^{-1}$) and % change
Li_2RuO_3	329.0
$Li_2Ru_{0.5}Ti_{0.5}Cr_0O_3$	393.19 (19.5%)
$Li_2Ru_{0.5}Ti_{0.375}Cr_{0.125}O_3$	391.70 (19.1%)
$Li_2Ru_{0.5}Ti_{0.25}Cr_{0.25}O_3$	390.23 (18.6%)
$Li_2Ru_{0.5}Ti_{0.125}Cr_{0.375}O_3$	388.77 (18.2%)
$Li_2Ru_{0.5}Ti_0Cr_{0.5}O_3$	387.32 (17.7%)

B. Formation Energy (FE)

The amount of energy required to form a cathode from its constituent elements in their normal states is referred as the Formation Energy (FE). The FE affects the stability of the cathode material in such a way that the stability of the cathode increases as the formation energy becomes more negative. The FE of the cathodes is calculated using the formula:

$$FE = E\left[Li_2Ru_{0.5}Ti_yCr_{05-y}O_3\right] - 2E[Li] - 0.5E[Ru] - yE[Ti] - (0.5-y)E[Cr] - \frac{3}{2}E[O_2] \quad (2)$$

where, FE is the formation energy of the cathode, $E\left[Li_2Ru_{0.5}Ti_yCr_{05-y}O_3\right]$ is the computed total energy of $Li_2Ru_{0.5}Ti_yCr_{05-y}O_3$ after geometry optimisation, $E[Li], E[Ru], E[Ti], E[Cr],$ and $E[O_2]$ are respectively the total energies of Li, Ru, Ti, Cr and O in their standard states.

Table 3 shows that all cathodes exhibit negative FE values, which suggests that the crystal structures of the cathodes under study are stable. Further, the FE of each co-doped cathode is higher than that of the parent LRO cathode. In other words, adding Ti and Cr together increases the formation energy, which makes the cathode's structure more stable. The cathode $Li_2Ru_{0.5}Ti_{0.375}Cr_{0.125}O_3$ is considered

most stable because it shows highest FE among all cathodes. The order of stability of cathodes based on the FE values is:

$Li_2Ru_{0.5}Ti_{0.375}Cr_{0.125}O_3$ > $Li_2Ru_{0.5}Ti_{0.25}Cr_{0.25}O_3$ > $Li_2Ru_{0.5}Ti_{0.125}Cr_{0.375}O_3$ > $Li_2Ru_{0.5}Ti_0Cr_{0.5}O_3$ > $Li_2Ru_{0.5}Ti_{0.5}Cr_0O_3$ > Li_2RuO_3

Table 3. Formation energies and percentage change of cathodes for different doping combinations calculated using the quantum mechanical methods

Cathode	Formation Energy (eV) and % change
Li_2RuO_3	-11.75
$Li_2Ru_{0.5}Ti_{0.5}Cr_0O_3$	-13.94 (18.6%)
$Li_2Ru_{0.5}Ti_{0.375}Cr_{0.125}O_3$	-15.10 (28.5%)
$Li_2Ru_{0.5}Ti_{0.25}Cr_{0.25}O_3$	-14.63 (24.5%)
$Li_2Ru_{0.5}Ti_{0.125}Cr_{0.375}O_3$	-14.29 (21.6%)
$Li_2Ru_{0.5}Ti_0Cr_{0.5}O_3$	-13.85 (17.9%)

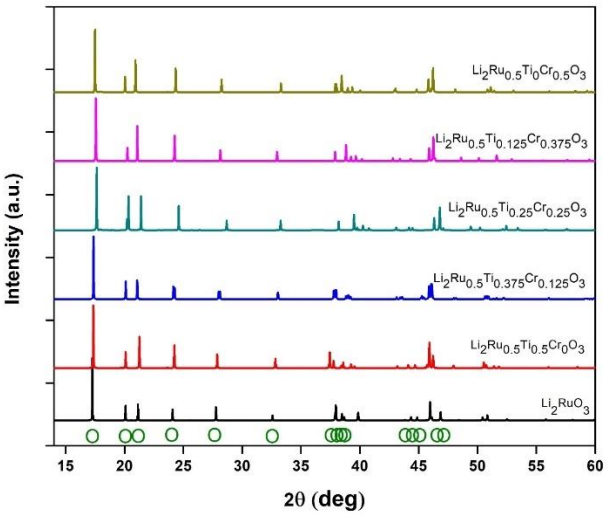

Figure 2. X-ray diffraction pattern of co-doped cathodes compared to that of the pristine Li_2RuO_3. The experimental data was shown in circles (green).

C. Powder X-ray Diffraction (XRD)

Figure 2 shows powder XRD patterns for LRO with and without Ti and Cr doping to compare their structural characteristics. Figure 2 shows that cathode XRD patterns are in good agreement with experimental data. The Bragg angles of the investigated cathodes and the observed peak positions are quite close, indicating that doping with Ti and Cr will not cause appreciable structural changes. In other words, the crystal structure remains stable after Ti and Cr co-doping.

D. Thermodynamic Stability

The thermodynamic stability of a battery is one of the crucial factors that assures its risk-free operation. Therefore, it is critical to examine its thermodynamic stability before employing them as a cathode in batteries. During the charging of the Li-ion battery, the LRO cathode decomposes according to the equation given below (Xiao *et al.*, 2012):

$$Li_xRu_{0.5}Ti_yCr_{0.5-y}O_3\ (lattice) \rightarrow Li_xRu_{0.5}Ti_yCr_{0.5-y}O_{3-z}\ (lattice) + \frac{z}{2}O_2\ (gas) \quad (3)$$

In multilayer LRO cathodes, the release of oxygen is one of the primary issues (Moradi *et al.*, 2020). This is because the oxygen evolution rate is directly related to the thermodynamic stability of the cathode. This reaction could ignite or explode the battery cathode. By limiting oxygen loss and stabilising oxygen inside the lattice, the lifetime and performance of cathode materials can be greatly enhanced.

To explore the thermodynamic stability in relation to oxygen evolution, the Gibbs free energy (ΔG) has been calculated for the cathodes at varying amounts (x) of Li using the well-known equation $\Delta G=\Delta H-TS$, where ΔH is the change in enthalpy. The value ΔH for a cathode is computed (S. Wang *et al.*, 2017; Yang *et al.*, 2017; H. Zhang *et al.*, 2019) using the following equation:

$$\Delta H(eV) = \frac{E(Li_xRu_{0.5}Ti_yCr_{0.5-y}O_{3-z}) + 0.5z\,E[O_2] - E(Li_xRu_{0.5}Ti_yCr_{0.5-y}O_3)}{0.5z} \quad (4)$$

where, E is the total energy obtained from DFT+U method.

By taking the findings of the preceding studies (Francis Amalraj *et al.*, 2012; H. Zhang *et al.*, 2019) into account, the value of TS was considered to be 0.63eV for the O_2 molecule when it was subjected to standard conditions of temperature and pressure. As a result, the Gibbs free energy (ΔG) associated with the LRO decomposition reaction (3) can be computed as (H. Zhang *et al.*, 2019; F. Zheng *et al.*, 2019).

$$\Delta G(eV) = \Delta H - 0.63 \quad (5)$$

During Li-ion battery charging, some electrons are removed from the cathode, lowering the ΔG of the reaction. A decrease in ΔG at a given temperature accelerates oxygen extraction from the reaction mixture and cathode degradation. If the cathode disintegrates faster, its

degradation temperature will become lower. This reduces reversible capacity, longevity, and safe operating range. If ΔG for extracted lithium ions is negative, the reaction will be spontaneous.

Figure 3 illustrates Gibbs free energy (ΔG) as a function of lithium removed from cathodes. Figure 3 shows that when x in Li_x[cathode] is lowered to 1.15, ΔG value of the LRO cathode becomes negative, indicating spontaneous oxygen removal. Similarly, ΔG becomes negative for the co-doped cathodes $Li_2Ru_{0.5}Ti_{0.5}Cr_0O_3$, $Li_2Ru_{0.5}Ti_{0.375}Cr_{0.125}O_3$, $Li_2Ru_{0.5}Ti_{0.25}Cr_{0.25}O_3$, $Li_2Ru_{0.5}Ti_{0.125}Cr_{0.375}O_3$, and $Li_2Ru_{0.5}Ti_0Cr_{0.5}O_3$ when x 0.80, 0.47, 0.60, 0.81, and 0.94, respectively.

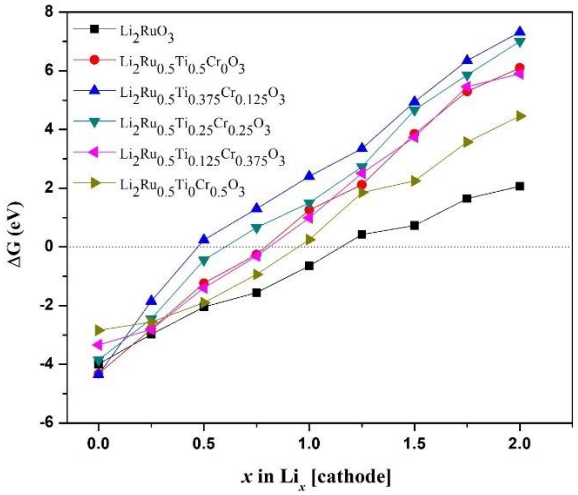

Figure 3. Calculated ΔG values for the oxygen elimination reaction at different Li-ion contents in the cathode materials

Co-doped cathodes have greater (ΔG values than LRO cathodes, indicating that breakdown requires higher temperatures. Thus, it is reasonable to assume, co-doped cathodes have a greater decomposition temperature than pristine LRO, resulting in enhanced reversible capacity and thermal stability. The thermal stability of the cathode structure under investigation are in the order of $Li_2Ru_{0.5}Ti_{0.375}Cr_{0.125}O_3$ > $Li_2Ru_{0.5}Ti_{0.25}Cr_{0.25}O_3$ > $Li_2Ru_{0.5}Ti_{0.5}Cr_0O_3$ > $Li_2Ru_{0.5}Ti_{0.125}Cr_{0.375}O_3$ > $Li_2Ru_{0.5}Ti_0Cr_{0.5}O_3$ > Li_2RuO_3. The cathode $Li_2Ru_{0.5}Ti_{0.375}Cr_{0.125}O_3$ exhibits highest decomposition temperature and thermal stability among the co-doped cathodes examined.

E. Voltage Stability

Maximum output power of a Lithium-ion battery depends on cell voltage, which depends on cathode and anode voltages. LRO has high open circuit voltage which makes it a significant cathode material. Dopants can cause this voltage to fluctuate, thus it is important to understand these changes. During charge-discharge cycles, when Li-solid is utilised as the anode in a LIB, the following reaction occurs:

$$Li_x[cathode] + (y - x)Li_{solid} \rightleftharpoons Li_y[cathode] \quad (6)$$

Here, x and y are Li-ion concentrations in the reactant and product states. As a result, the open-circuit voltage of the LIB at different Li concentrations in the cathode can be obtained by the following equation (Goodenough & Park, 2013; Medasani *et al.*, 2016):

$$V_{OC} = \frac{-\Delta\mu}{F} = \frac{\Delta E}{y-x} = \frac{E_{Li_y} - [E_{Li_x} + (y-x)E_{Li_{solid}}]}{y-x} \quad (7)$$

where E is the total energy of the material obtained with DFT PBE+U calculations, μ is chemical potential (eV) and F is Faraday constant (C mol^{-1}).

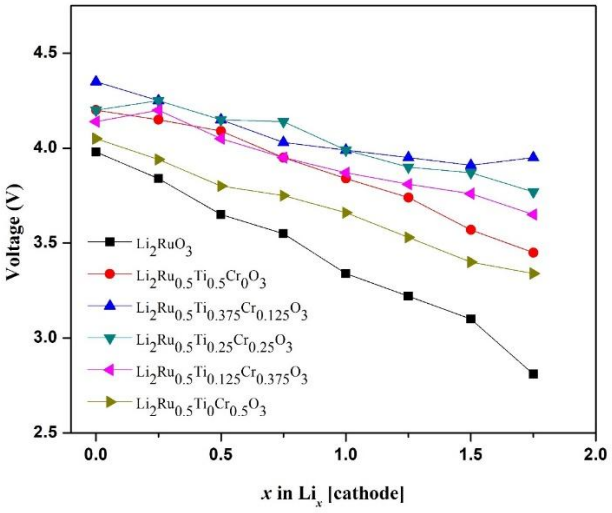

Figure 4. The calculated open circuit voltages of cathode materials at different Li-ion contents

Figure 4 compares co-doped and undoped LRO cathode open-circuit voltages. Maximum open-circuit voltage is reached when all Li-ions are withdrawn from the cathode. The maximum voltage for an undoped LRO cathode is 3.98V, while the maximum voltage for co-doped cathodes $Li_2Ru_{0.5}Ti_{0.5}Cr_0O_3$, $Li_2Ru_{0.5}Ti_{0.375}Cr_{0.125}O_3$, $Li_2Ru_{0.5}Ti_{0.25}Cr_{0.25}O_3$, $Li_2Ru_{0.5}Ti_{0.125}Cr_{0.375}O_3$, and $Li_2Ru_{0.5}Ti_0Cr_{0.5}O_3$ is 4.2, 4.35, 4.2, 4.14, and 4.05V respectively. Calculations indicate that co-doping with Ti and

Cr raises the maximum voltage of pure LRO by at least 1.7%. $Li_2Ru_{0.5}Ti_{0.375}Cr_{0.125}O_3$ has the highest maximum voltage (4.35V) among co-doped cathodes, which is approximately 9.3% greater than that of pure LRO cathode. Regardless of Li concentration, co-doped cathodes have higher open circuit voltages than undoped LRO.

Table 4. The voltage reduction values and percentage changes of the studied cathode materials extracted from the open circuit voltage plots in Figure 4

Cathode	**Voltage Reduction (V) and percentage change**
Li_2RuO_3	1.17
$Li_2Ru_{0.5}Ti_{0.5}Cr_0O_3$	0.75 (35.9%)
$Li_2Ru_{0.5}Ti_{0.375}Cr_{0.125}O_3$	0.40 (65.8%)
$Li_2Ru_{0.5}Ti_{0.25}Cr_{0.25}O_3$	0.43 (63.2%)
$Li_2Ru_{0.5}Ti_{0.125}Cr_{0.375}O_3$	0.49 (58.1%)
$Li_2Ru_{0.5}Ti_0Cr_{0.5}O_3$	0.71 (39.3%)

Voltage trend shown from Figure 4 represents the voltage stability of cathodes. When the Li-ion content is altered from $x = 0$ to $x = 1.8$, it is seen that the voltages significantly drop. The voltage drops for each cathode as a function of variation in Li-ions from $x = 0$ to $x = 1.8$ is presented in Table 4. The cut-off voltage, lowest operational voltage, is achieved more rapidly with higher voltage reduction. As a result, the voltage stability declines, lowering the usable capacity. Table 4 shows that, compared to the pristine LRO, all co-doped cathode materials undergo reduced voltage reduction. The voltage reduction of pure LRO is 1.17V, but for the co-doped cathodes $Li_2Ru_{0.5}Ti_{0.5}Cr_0O_3$, $Li_2Ru_{0.5}Ti_{0.375}Cr_{0.125}O_3$, $Li_2Ru_{0.5}Ti_{0.25}Cr_{0.25}O_3$, $Li_2Ru_{0.5}Ti_{0.125}Cr_{0.375}O_3$, and $Li_2Ru_{0.5}Ti_0Cr_{0.5}O_3$, it is, respectively, 0.75, 0.40, 0.43, 0.49, and 0.71V. The co-doped cathodes consequently have improved voltage stability and practical capacity. The voltage drop is greatly reduced by co-doping with Ti and Cr by at least 35.9%, with $Li_2Ru_{0.5}Ti_{0.375}Cr_{0.125}O_3$ experiencing the greatest reduction (65.8%). These findings demonstrate a considerable improvement in the voltage stability and usable capacity of the LRO cathode due to co-doping with Ti and Cr.

F. Bandgap

Bandgap is an important characteristic that can affect the electrical conductivity of a cathode. Consequently, it is crucial to comprehend the influence of co-doping on the LRO bandgap, since this can help to explain the difference in its electrical conductivity.

Table 5. The calculated bandgaps of the studied cathode materials and percentage change in the bandgap when compared to the pristine Li_2RuO_3

Cathode	**Bandgap (eV) and % change**
Li_2RuO_3	0.51
$Li_2Ru_{0.5}Ti_{0.5}Cr_0O_3$	0.42 (17.6%)
$Li_2Ru_{0.5}Ti_{0.375}Cr_{0.125}O_3$	0.33 (35.3%)
$Li_2Ru_{0.5}Ti_{0.25}Cr_{0.25}O_3$	0.38 (25.5%)
$Li_2Ru_{0.5}Ti_{0.125}Cr_{0.375}O_3$	0.43 (15.7%)
$Li_2Ru_{0.5}Ti_0Cr_{0.5}O_3$	0.46 (9.8%)

The bandgaps of undoped LRO and co-doped LRO cathodes are shown in Table 5. According to Table 5, the band gap of undoped LRO is 0.51eV, which is consistent with previous studies (Johannes *et al.*, 2008; Pchelkina *et al.*, 2015). The co-doped cathodes $Li_2Ru_{0.5}Ti_{0.5}Cr_0O_3$, $Li_2Ru_{0.5}Ti_{0.375}Cr_{0.125}O_3$, $Li_2Ru_{0.5}Ti_{0.25}Cr_{0.25}O_3$, $Li_2Ru_{0.5}Ti_{0.125}Cr_{0.375}O_3$, and $Li_2Ru_{0.5}Ti_0Cr_{0.5}O_3$ have bandgaps of 0.42, 0.33, 0.38, 0.43, and 0.46 eV respectively. These findings demonstrate that co-doping with Ti and Cr reduces the bandgap by at least 9.8%. Among the examined cathodes, $Li_2Ru_{0.5}Ti_{0.375}Cr_{0.125}O_3$ has the smallest bandgap, which is approximately 35.3% smaller than the pure LRO cathode. Pristine LRO cathode will have the lowest electrical conductivity compared to co-doped cathodes due to its higher bandgap indicating that co-doping boosts the electrical conductivity substantially. On the basis of bandgap values, the expected descending order of electrical conductivity of examined cathodes is as follows:

$Li_2Ru_{0.5}Ti_{0.375}Cr_{0.125}O_3$ > $Li_2Ru_{0.5}Ti_{0.25}Cr_{0.25}O_3$ > $Li_2Ru_{0.5}Ti_{0.5}Cr_0O_3$ > $Li_2Ru_{0.5}Ti_{0.125}Cr_{0.375}O_3$ > $Li_2Ru_{0.5}Ti_0Cr_{0.5}O_3$ > Li_2RuO_3

IV. CONCLUSION

In conclusion, DFT+U quantum mechanical calculations were used to examine the influence of Ti and Cr co-doping on parameters that can influence the electrochemical performance of Li_2RuO_3. The key findings from the DFT+U quantum mechanical calculations of co-doped LRO are presented below:

1. Co-doping with Ti and Cr improves the theoretical charge capacity of LRO by at least 17.7% and $Li_2Ru_{0.5}Ti_{0.5}Cr_0O_3$ has the highest capacity.
2. Formation energy of co-doped cathodes is higher than that of pristine LRO by at least 17.9% with $Li_2Ru_{0.5}Ti_{0.375}Cr_{0.125}O_3$ showing the highest formation energy of -15.10 eV.
3. Co-doping with Ti and Cr does not lead to appreciable crystal structural changes.
4. Co-doped cathodes have higher decomposition temperatures in comparison to the undoped LRO, resulting in larger reversible capacity and superior thermal stability. The cathode $Li_2Ru_{0.5}Ti_{0.375}Cr_{0.125}O_3$ exhibits highest thermal stability.
5. The maximum voltage of undoped LRO is increased by at least 1.7% when co-doped with Ti and Cr. The maximum voltage of the co-doped cathode $Li_2Ru_{0.5}Ti_{0.375}Cr_{0.125}O_3$ is 4.35V, which is around 9.3% higher than the voltage of the undoped LRO cathode.
6. Co-doping with Ti and Cr reduces voltage drop by at least 35.9%, with the greatest drop achieved in $Li_2Ru_{0.5}Ti_{0.375}Cr_{0.125}O_3$ (65.8%).
7. The bandgap is reduced by at least 9.8% when Ti and Cr are co-doped. Among the cathodes under study, $Li_2Ru_{0.5}Ti_{0.375}Cr_{0.125}O_3$ has the lowest bandgap (0.33eV), which is almost 35.3 % lower than the undoped LRO cathode.

V. ACKNOWLEDGEMENTS

One of the authors, C. Bapanayya would like to thank Dr. N. Parvathala Reddy for his support during the development of the manuscript.

VI. REFERENCES

Aasen, D, Michael, PC & Douglas, GI 2020, 'Investigation of Transition Metal-Based (Mn, Co, Ni, Fe) Trimetallic Oxide Nanoparticles on N-Doped Carbon Nanotubes as Bifunctional Catalysts for Zn-Air Batteries', Journal of The Electrochemical Society, vol. 167, no. 4, p. 40503. doi: 10.1149/1945-7111/ab7094.

Afyon, S, Michael, W & Reinhard, N 2013, 'A Lithium-Rich Compound $Li_7Mn(BO_3)_3$ Containing Mn^{2+} in Tetrahedral Coordination: A Cathode Candidate for Lithium-Ion Batteries', Angewandte Chemie - International Edition.

Anisimov, VI, Aryasetiawan, F & Lichtenstein, AI 1997, 'First-Principles Calculations of the Electronic Structure and Spectra of Strongly Correlated Systems: The LDA/U Imethod', Journal of Physics: Condensed Matter, vol. 9, no. 4, pp. 767–808. doi: 10.1088/0953-8984/9/4/002.

Arunkumar, P, Jin Jeong, W, Won, S & Bin Im, W 2016, 'Improved Electrochemical Reversibility of Over-Lithiated Layered Li_2RuO_3 Cathodes: Understanding Aliovalent Co^{3+} Substitution with Excess Lithium', Journal of Power Sources, vol. 324, pp. 428–38. doi: 10.1016/j.jpowsour.2016.05.013.

Aryasetiawan, F, Karlsson, K, Jepsen, O & Schönberger, U 2006, 'Calculations of Hubbard-U from First-Principles', Physical Review B, vol. 74. no. 12, p. 125106. doi: 10.1103/PhysRevB.74.125106.

Francis Amalraj, S *et al.* 2012, 'Study of the Electrochemical Behavior of the 'Inactive' Li_2MnO_3', Electrochimica Acta, vol. 78, pp. 32–39, <https://www.sciencedirect.com/science/article/pii/S0013468612009802>.

Gao, Yurui *et al.* 2015, 'Selecting Substituent Elements for Li-Rich Mn-Based Cathode Materials by Density Functional Theory (DFT) Calculations', Chemistry of Materials, vol. 27, no. 9, pp. 3456–61. doi: 10.1021/acs.chemmater.5b00875.

Goodenough, John, B & Sung Park, K 2013, 'The Li-Ion Rechargeable Battery: A Perspective', Journal of the American Chemical Society.

He, Xiaoshu *et al.* 2019, 'Improved Electrochemical Performance of $LiNi_{0.8}Co_{0.15}Al_{0.05}O_2$ Cathode Material by

Coating of Graphene Nanodots', Journal of The Electrochemical Society, vol. 166, no. 6, pp. A1038–A1044. doi: 10.1149/2.0541906jes.

James, ACWP & Goodenough, JB 1988, 'Structure and Bonding in Lithium Ruthenate, Li_2RuO_3,' Journal of Solid State Chemistry, vol. 74, no. 2, pp. 287–94.

Johannes, MD, Stux, AM & Swider-Lyons, KE 2008, 'Electronic Structure and Properties of Li-Insertion Materials: Li_2RuO_3 and RuO_2', Physical Review B, vol. 77, no. 7, p. 75124. doi: 10.1103/PhysRevB.77.075124.

Johnson, CS *et al.* 2010, 'Li_2O Removal from Li_5FeO_4: A Cathode Precursor for Lithium-Ion Batteries', Chemistry of Materials.

Kalantarian, Mohammad Mahdi, Sirous Asgari & Piercarlo Mustarelli 2013, 'Theoretical Investigation of Li_2MnSiO_4 as a Cathode Material for Li-Ion Batteries: A DFT Study', J. Mater. Chem. A, vol. 1, no. 8, pp. 2847–55. doi: 10.1039/C2TA01363K.

Kalathil, Abdul Kareem *et al.* 2015, 'Influence of Ti^{4+} on the Electrochemical Performance of Li-Rich Layered Oxides - High Power and Long Cycle Life of $Li_2Ru_{1-X}Ti_XO_3$ Cathodes', ACS Applied Materials & Interfaces, vol. 7, no. 13, pp. 7118–28. doi: 10.1021/am507951x.

Lanjan, Amirmasoud, Behnam, GC & Sepideh, A-I 2020a, 'First Principle Study on the Application of Crystalline Cathodes $Li_2Mn_{0.5}TM_{0.5}O_3$ for Promoting the Performance of Lithium-Ion Batteries', Computational Materials Science, vol. 173, p. 109417. <https://www.sciencedirect.com/science/article/pii/S0927025619307165>.

——— 2020b, 'Promoting Lithium-Ion Battery Performance by Application of Crystalline Cathodes $Li_xMn_{1-z}Fe_zPO_4$', Journal of Solid State Electrochemistry, vol. 24, no. 1, pp. 157–71. doi: 10.1007/s10008-019-04480-6.

Li, Qi *et al.* 2015, 'Balancing Stability and Specific Energy in Li-Rich Cathodes for Lithium Ion Batteries: A Case Study of a Novel Li–Mn–Ni–Co Oxide', J. Mater. Chem. A, vol. 3, no. 19, pp. 10592–602. doi: 10.1039/C5TA00929D.

Liu, Shengzhou *et al.* 2017, 'Chromium Doped Li_2RuO_3 as a Positive Electrode with Superior Electrochemical Performance for Lithium Ion Batteries', Chemical Communications, vol. 53, no. 87, pp. 11913–16. doi: 10.1039/C7CC07545F.

Lu, Languang *et al.* 2013, 'A Review on the Key Issues for Lithium-Ion Battery Management in Electric Vehicles', Journal of Power Sources, vol. 226, pp. 272–88.

Medasani, B *et al.* 2016, 'Predicting Defect Behavior in B2 Intermetallics by Merging Ab Initio Modeling and Machine Learning', npj Computational Materials, vol. 2, no. 1, p. 1. doi: 10.1038/s41524-016-0001-z.

Mizushima, K, Jones, PC, Wiseman, PJ & Goodenough, JB 1981, 'Li_xCoO_2 ($0<x\leq1$): A New Cathode Material for Batteries of High Energy Density', Solid State Ionics, vol. 3–4(C), pp. 171–74.

Momma, K & Fujio, I 2011, 'VESTA 3 for Three-Dimensional Visualization of Crystal, Volumetric and Morphology Data', Journal of Applied Crystallography, vol. 44, no. 6, pp. 1272–76.

Moradi, Z, Amirmasoud, L & Seshasai, S 2020, 'Enhancement of Electrochemical Properties of Lithium Rich Li_2RuO_3 Cathode Material', Journal of The Electrochemical Society, vol. 167, no. 11.

——— 2021, 'Multiscale Investigation into the Co-Doping Strategy on the Electrochemical Properties of Li_2RuO_3 Cathodes for Li-Ion Batteries', ChemElectroChem, vol. 8, no. 1, pp. 112–24. doi: 10.1002/celc.202001206.

Nkosi, Funeka P *et al.* 2017, 'Insights into the Synergistic Roles of Microwave and Fluorination Treatments towards Enhancing the Cycling Stability of P2-Type $Na_{0.67}[Mg_{0.28}Mn_{0.72}]O_2$ Cathode Material for Sodium-Ion Batteries', Journal of The Electrochemical Society, vol. 164, no. 13, pp. A3362–A3370. doi: 10.1149/2.1721713jes.

Okumura, T, Shikano, M & Kobayashi, H 2014, 'Effect of Bulk and Surface Structural Changes in Li_5FeO_4 Positive Electrodes during First Charging on Subsequent Lithium-Ion Battery Performance', Journal of Materials Chemistry A.

Padhi, AK 1997, 'Phospho-Olivines as Positive-Electrode Materials for Rechargeable Lithium Batteries', Journal of The Electrochemical Society, vol. 144, no. 4, p. 1188.

Pang, Shengli *et al.* 2018, 'Enhanced Electrochemical Performance of $Li_{1.2}Mn_{0.54}Ni_{0.13}Co_{0.13}O_2$ via L-Ascorbic Acid-Based Treatment as Cathode Material for Li-Ion Batteries', Journal of The Electrochemical Society, vol. 165, no. 9, pp. A1897–A1902. doi: 10.1149/2.1481809jes.

Park, Min-Sik *et al.* 2013, 'Li_2RuO_3 as an Additive for High-Energy Lithium-Ion Capacitors', The Journal of Physical Chemistry C, vol. 117, no. 22, pp. 11471–78. doi: 10.1021/jp4005828.

Pchelkina, ZV *et al.* 2015, 'Electronic Structure of Li_2RuO_3 Studied by LDA and LDA+DMFT Calculations and Soft X-Ray Spectroscopy', Physical Review B, vol. 91, no. 11, p. 115138, <https://link.aps.org/doi/10.1103/PhysRevB.91.115138>.

Perdew, JP, Burke, K & Matthias, E 1996, 'Generalized Gradient Approximation Made Simple', Physical Review Letters, vol. 77, no. 18, pp. 3865–68. doi: 10.1103/PhysRevLett.77.3865.

Song, Bohang *et al.* 2015, 'Nano-Structural Changes in Li-Ion Battery Cathodes during Cycling Revealed by FIB-SEM Serial Sectioning Tomography', J. Mater. Chem. A, vol. 3, no. 35, pp. 18171–79. doi: 10.1039/C5TA04151A.

Su, Yuefeng *et al.* 2020, 'Enhanced High-Temperature Performance of Li-Rich Layered Oxide via Surface Heterophase Coating', Journal of Energy Chemistry, vol. 51, pp. 39–47, <https://www.sciencedirect.com/science/article/pii/S2095495620301650>.

Tian, Xiaoqing *et al.* 2019, 'A New Lithium-Rich Layer-Structured Cathode Material with Improved Electrochemical Performance and Voltage Maintenance', International Journal of Energy Research, vol. 43, no. 13, pp. 7547–56. <https://onlinelibrary.wiley.com/doi/abs/10.1002/er.4724>.

Torres-Castro, L, Abreu-Sepulveda, MA, Katiyar, RS & Manivannan, A 2017, 'Electrochemical Investigations on the Effect of Mg-Substitution in Li_2MnO_3 Cathode', Journal of The Electrochemical Society, vol. 164, no. 7, pp. A1464–A1473. doi: 10.1149/2.0661707jes.

Wang, Jiexi *et al.* 2018, '$Li_3V(MoO_4)_3$ as a Novel Electrode Material with Good Lithium Storage Properties and Improved Initial Coulombic Efficiency', Nano Energy, vol. 44, pp. 272–78.

Wang, S, Liu, J & Sun, Q 2017, 'New Allotropes of Li_2MnO_3 as Cathode Materials with Better Cycling Performance Predicted in High Pressure Synthesis', Journal of Materials Chemistry A, vol. 5, no. 32, pp. 16936–43. doi: 10.1039/C7TA04941B.

Wu, Feng *et al.* 2020, 'Renovating the Electrode-Electrolyte Interphase for Layered Lithium- & Manganese-Rich Oxides', Energy Storage Materials, vol. 28, pp. 383–92, <https://www.sciencedirect.com/science/article/pii/S2405829719310955>.

Xiao, P, Deng, ZQ, Manthiram, A & Henkelman, G 2012, 'Calculations of Oxygen Stability in Lithium-Rich Layered Cathodes', The Journal of Physical Chemistry C, vol. 116, no. 44, pp. 23201–4. doi: 10.1021/jp3058788.

Xu, Ming *et al.* 2015, 'Mitigating Capacity Fade by Constructing Highly Ordered Mesoporous Al_2O_3/Polyacene Double-Shelled Architecture in Li-Rich Cathode Materials', J. Mater. Chem. A, vol. 3, no. 26, pp. 13933–45. doi: 10.1039/C5TA03676C.

Yang, MY *et al.* 2017, 'Role of Ordered Ni Atoms in Li Layers for Li-Rich Layered Cathode Materials', Advanced Functional Materials, vol. 27, no. 35, p. 1700982. doi: 10.1002/adfm.201700982.

Yanxia, Sun *et al.* 2020, 'Improved Lithium Ion Diffusion and Stability of a $LiNi_{0.8}Co_{0.1}Mn_{0.1}O_2$ Cathode via the Synergistic Effect of Na and Mg Dual-Metal Cations for Lithium Ion Battery', Journal of The Electrochemical Society, vol. 167, no. 2, p. 20522. doi: 10.1149/1945-7111/ab6977.

Ye, Delai *et al.* 2014, 'Understanding the Stepwise Capacity Increase of High Energy Low-Co Li-Rich Cathode Materials for Lithium Ion Batteries', J. Mater. Chem. A, vol. 2, no. 44, pp. 18767–74. doi: 10.1039/C4TA03692A.

Zhang, Hongliang *et al.* 2019, 'Selecting Substituent Elements for $LiMnPO_4$ Cathode Materials Combined with Density Functional Theory (DFT) Calculations and Experiments', Journal of Alloys and Compounds, vol. 793, pp. 360–68, <https://www.sciencedirect.com/science/article/pii/S092583881931480X>.

Zhang, YL, Fan, H & Han, M 2018, 'Stability of Ni-YSZ Anode for SOFCs in Methane Fuel: The Effects of Infiltrating Lasub0.8/SubSrsub0.2/SubFeOsub3-/Suband Gd-Doped CeOsub2/SubMaterials', Journal of The Electrochemical Society, vol. 165, no. 10, pp. F756–F763. doi: 10.1149/2.0171810jes.

Zheng, Feng *et al.* 2019, 'Impact of Structural Transformation on Electrochemical Performances of Li-Rich Cathode Materials: The Case of Li_2RuO_3, Journal of Physical Chemistry C, vol. 123, no. 22, pp. 13491–99.

Zheng, Shiyao *et al.* 2019, 'Novel Ordered Rocksalt-Type Lithium-Rich $Li_2Ru_{1-X}Ni_XO_{3-\delta}$ ($0.3 \leq x \leq 0.5$) Cathode Material with Tunable Anionic Redox Potential', ACS Applied Energy Materials, vol. 2, no. 8, pp. 5933–44. doi: 10.1021/acsaem.9b01051.

Zhi, Mingjia *et al.* 2013, 'Nanostructured Carbon–Metal Oxide Composite Electrodes for Supercapacitors: A Review', Nanoscale, vol. 5, no. 1, pp. 72–88. doi: 10.1039/C2NR32040A.